December 2003

IFIC/03-55
FTUV-03-1205

Neutrino oscillation physics with a higher γ β-beam

J. Burguet-Castell[a,1] D. Casper[b,2], J.J. Gómez-Cadenas[a,3], P. Hernández[a,4] F. Sánchez[c,5]

[a] *Departamento de Física Teórica and IFIC, Universidad de València, E-46100 Burjassot, Spain*

[b] *Department of Physics and Astronomy, University of California, Irvine CA 92697-4575, USA*

[c] *IFAE, Universidad Autonoma de Barcelona, E-08193 Bellaterra, Barcelona.*

Abstract

The precision measurement and discovery potential of a neutrino factory based on boosted radioactive ions in a storage ring ("β-beam") is re-examined. In contrast with past designs, which assume ion γ factors of ~ 100 and baselines of $L = 130$ km, we emphasize the advantages of boosting the ions to higher γ and increasing the baseline proportionally. In particular, we consider a "medium-"γ scenario ($\gamma \sim 500$, $L \sim 730$ km) and a "high-"γ scenario ($\gamma \sim 2000$, $L \sim 3000$ km). The increase in statistics, which grow linearly with the average beam energy, the ability to exploit the energy dependence of the signal and the sizable matter effects at this longer baseline all increase the discovery potential of such a machine very significantly.

[1] jordi.burguet-castell@cern.ch
[2] dcasper@uci.edu
[3] gomez@mail.cern.ch
[4] pilar.hernandez@cern.ch
[5] fsanchez@ifae.es

1. Introduction

The spectacular results in atmospheric [1], solar [2], reactor [3] and long-baseline [4] neutrino experiments in recent years can be economically accommodated in the Standard Model (SM) with neutrino masses and a three-neutrino mixing matrix [5]. In this case, the lepton sector of the SM closely resembles that of the quarks and there are a number of new physical parameters that can be measured at low energies: the three neutrino masses, m_i ($i = 1, 2, 3$), three mixing angles, θ_{ij}, ($i \neq j = 1, 2, 3$), and a CP violating phase, δ. In contrast with the quark sector two additional phases could be present if neutrinos are Majorana. Of all these new parameters, present experiments have determined just two neutrino mass-square differences and two mixing angles: ($|\Delta m^2_{23}| \simeq 2.5 \times 10^{-3}$ eV^2, $\theta_{23} \simeq 45^\circ$) which mostly drive the atmospheric oscillation and ($\Delta m^2_{12} \simeq 7 \times 10^{-5}$ eV^2, $\theta_{12} \simeq 35^\circ$) which mostly drive the solar one. The third angle, θ_{13}, as well as the CP-violating phases (δ, and possible Majorana phases) remain undetermined. Another essential piece of information needed to clarify the low-energy structure of the lepton flavor sector of the SM is the neutrino mass hierarchy. This is related to the sign of the largest mass-square difference (Δm^2_{23}), which determines if the spectrum is hierarchical (if the two most degenerate neutrinos are lighter than the third one) or degenerate (if they are heavier).

The measurement of these parameters requires, for the first time, high-precision neutrino-oscillation experiments. A number of possible experimental setups to significantly improve the present sensitivity to θ_{13}, δ and the sign of Δm^2_{23} have been discussed in the literature: neutrino factories (neutrino beams from boosted-muon decays) [6], superbeams (very intense conventional neutrino beams) [7, 8, 9] improved reactor experiments [10] and more recently β-beams (neutrinos from boosted-ion decays) [11, 12]. These are quite different in terms of systematics but all face a fundamental problem which limits the reach of each individual experiment significantly, namely the problem of correlations and degeneracies between parameters [13]-[19]; θ_{13} and δ must be measured simultaneously, and other oscillation parameters are not known with infinite precision.

To resolve these degeneracies it is important to measure as many independent channels as possible and to exploit the energy and/or baseline dependence of the oscillation signals and matter effects in neutrino propagation. In many cases, the best way to do this is by combining different experiments; indeed the synergies between some combinations of the setups mentioned above have been shown to be very large.

The neutrino factory is thought to provide ultimate sensitivity to leptonic CP violation, and thus has been considered for a long time as the last step on a long-term road map to reveal the lepton-flavor sector of the SM. In this road map there are important intermediate milestones, such as superbeams or improved reactor experiments, that can mitigate the problem of degeneracies. In contrast, the present conception of the β-beam, which shares many of the good properties of the neutrino factory, has been shown to provide a rather limited sensitivity.

The purpose of this paper is to show that, in fact, a β-beam running at a higher γ than previously considered (and longer baselines), in combination with a massive water detector, can reach sensitivity to leptonic CP-violation and the sign(Δm^2_{23}) that competes with that in a neutrino factory. On the other hand, the R&D effort required to increase the γ factor for the β-beam setup is probably much less than that required to realize a high-energy, high-luminosity neutrino factory. Thus, an optimized β-beam may turn out to be a serious competitor to the neutrino factory as the "ultimate machine" to search for CP violation.

The paper is organized as follows. In Section 2 we recall a few facts about the present design for the β-beam and discuss the advantages of increasing the ion γ factor and the baseline. We also discuss the expected fluxes and event rates for three reference setups that will be considered for comparison, at low, medium and high γ. In Section 3, the performance of a large water Cerenkov apparatus, proposed as the optimal detector for the low and medium γ setups is discussed in detail. Sections 4 and 5 compare the physics results of the three reference setups. In Section 6 we present our outlook and conclusions.

2. The β-beam

The β-beam concept was first introduced in [11]. It involves producing a beam of β-unstable heavy ions, accelerating them to some reference energy, and allowing them to decay in the straight section of a storage ring, resulting in a very intense neutrino beam. Two ions have been identified as ideal candidates: ^{6}He, to produce a pure $\bar{\nu}_e$ beam, and ^{18}Ne, to produce a ν_e beam. The golden subleading transitions $\nu_e \to \nu_\mu$ and $\bar{\nu}_e \to \bar{\nu}_\mu$ can be measured through the appearance of muons in a distant detector.

As in the case of muon-induced neutrino beams, the $\beta-$beam offers the unique features of being *pure* (e.g., only one neutrino species, in contrast to a conventional super-beam where contamination of other neutrino species is inevitable) and virtually *systematics free*, since the spectrum can be calculated exactly (again, in contrast with a conventional beam, where knowledge of the spectrum always involves a sizable systematic uncertainty).

One of the most attractive features of the β-beam is that it leverages existing CERN facilities. The present design, whose feasability with existing technology has been recently demonstrated [20], envisions a "low-"γ scenario, in which ions are produced by a new facility (EURISOL), accelerated by the present SPS to $\gamma \leq 150$, and stored in a storage ring (also a new facility) with straight sections pointing to the experimental area. An underground location where a very massive neutrino dectector could be located has been identified in the Fréjus tunnel, roughly 130 km from CERN. This baseline is ideal for exploring the first peak of the atmospheric oscillation, the optimal environment to search for CP-violating effects. A new, very large cavern excavated in the Fréjus tunnel would host a megaton water Cerenkov detector a là UNO. The capabilities of such a detector are well-matched to this energy range, and the low neutrino energies produced by the low-γ option (in the range of a few hundred

MeV) require a very large mass to compensate for the tiny cross-sections.

Furthermore, the existing design calls for a conventional low-energy "super-beam" based on the proposed SPL proton driver [21], that would deliver a total power-on-target of about 4 MW, resulting in a very intense neutrino beam. The physics reach of such a super-beam has been studied in detail, both alone [9], and together with a low-γ $\beta-$beam [12, 22]. The results of these studies can be summarized as follows:

- Neither the SPL super-beam nor the low-γ $\beta-$beam, by themselves, result in fully-satisfactory performance, especially compared to other proposed facilities such as T2K at JPARC [7]. The performance is limited, in spite of the large detector mass by the small cross-sections, by systematics due to the SPL super-beam backgrounds (both beam- and detector-related) and by the intrinsic degeneracies identified in [14].

- A combination of the super-beam and β-beam would explore a large range of the parameter space (θ_{13}, δ). A detailed study of the systematics involved (in particular the absolute flux normalization of the SPL super-beam and the uncertainties in background subtraction) remains to be done, however. On-going studies in the context of the T2K project suggest that these systematics are not small.

- The sign of the atmospheric Δm^2_{23} cannot be determined because matter effects are negligible.

Here, instead, we explore increasing the energy of the β-beam, with a corresponding increase in baseline to keep $\langle E_\nu \rangle / L$ approximately constant. There are three reasons to expect an improvement of sensitivity in this case:

- The rates (and thus sensitivity to θ_{13} if the backgrounds are kept under control) increase linearly with $\langle E_\nu \rangle$ at fixed $\langle E_\nu \rangle / L$.

- At longer baselines, measurement of the neutrino mass hierarchy becomes possible, as matter effects become more sizable. This is illustrated in Figure 1, which shows the $\nu_e \to \nu_\mu$ oscillation probability for neutrinos and anti-neutrinos, as a function of the baseline, for neutrino energy constrained to the first atmospheric peak, i.e. $E/L = |\Delta m^2_{23}|/2\pi$. The difference between the neutrino and anti-neutrino oscillation probabilities induced by matter effects becomes comparable to that due to CP-violation for $L = \mathcal{O}(1000) km$.

- Increased neutrino energy enhances the energy dependence of oscillation signals. This is extremely useful in resolving the correlations and degeneracies in parameter space [13, 14]. Energy dependence is particularly helpful for energies close to the peak of the atmospheric oscillation [18], which is precisely the regime under consideration. Figure 2 compares the vacuum probabilities for $\nu_e \to \nu_\mu$ and $\bar{\nu}_e \to \bar{\nu}_\mu$ with $\theta_{13} = 6^\circ$ and $\delta = 40^\circ$ to those of the intrinsic-degenerate solution at $\langle E_{\nu(\bar{\nu})} \rangle$. The neutrino and anti-neutrino probabilities cross at the $\langle E_{\nu(\bar{\nu})} \rangle$, but are quite different at other energies. Thus spectral information can definitely help in disentangling them.

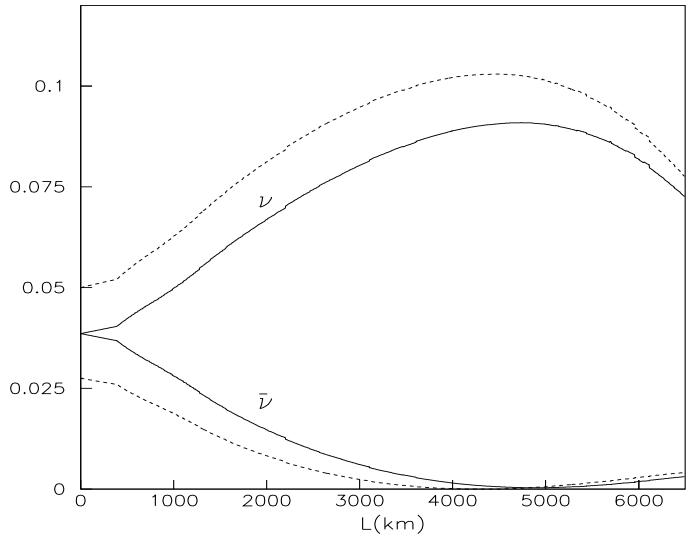

Figure 1: $P(\nu_e \to \nu_\mu)$ and $P(\bar{\nu}_e \to \bar{\nu}_\mu)$ as a function of the baseline L in km, at a neutrino energy $E/L = |\Delta m^2_{23}|/2\pi$ and for $\theta_{13} = 8^\circ$ and $\delta = 0$ (solid) and 90° (dashed).

From a technical point of view, designs aiming at higher γ factors are conceivable by direct extrapolation of existing technology, and would not require a long R&D program. A "medium-"γ scenario ($\gamma \leq 600$) could be realized at CERN by accelerating ions in a refurbished SPS with super-conducting magnets, or in LHC (up to γ =2488 for ^{6}He and $\gamma = 4158$ for ^{18}Ne) [23]. Another candidate would be Fermilab, where a combination of the existing Main-Injector and Tevatron could accelerate ions to γ factors of a few hundred.

The possibility of an associated super-beam[6] will not be considered here, because the systematics are very different. To gain a clear view of the relative merits of each $\beta-$beam scenario, it is best to first compare their stand-alone performance. Three scenarios for the $\beta-$beam *alone* are considered, and a future paper will address comparisons and combinations with other facilities. We define the following three setups:

- Setup I, low energy: $\gamma = 60$ for ^{6}He and $\gamma = 100$ for ^{18}Ne, with $L = 130$ km (CERN–Fréjus) as in [12, 22]. [7]

- Setup II, medium energy: $\gamma = 350$ for ^{6}He and $\gamma = 580$ for ^{18}Ne, with $L = 732$ km

[6]Note that it is also possible to increase the energy of the super-beam in the present design, by incresing the energy of the SPL.

[7]Different γ for ^{6}He and ^{18}Ne are required to allow simultaneous acceleration and storage of both ions in the same ring, reducing the necessary running time by a factor of two. The different ion charge:mass ratios imply a 1.67 ratio of γ factors [23].

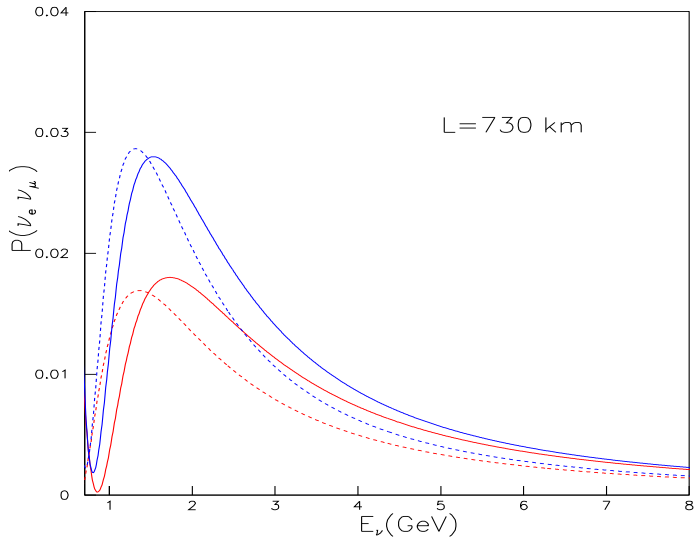

Figure 2: $P(\nu_e \to \nu_\mu)$ and $P(\bar{\nu}_e \to \bar{\nu}_\mu)$ as a function of the energy in GeV, at $L = 730$ km, for $\theta_{13} = 6^\circ$ and $\delta = 40^\circ$ (solid) and for the degenerate solution at $\theta'_{13}(\langle E_\nu \rangle), \delta'(\langle E_\nu \rangle)$ with $\langle E_\nu \rangle = 1.5$ GeV (dashed).

(e.g. CERN–Gran Sasso with a refurbished SPS or with the LHC, FNAL–Soudan with Tevatron).

- Setup III, high energy: $\gamma = 1500$ for ^{6}He and $\gamma = 2500$ for ^{18}Ne, with $L = 3000$ km (e.g. CERN–Canary islands with the LHC).

In all cases we assume the same number of ions as the existing design, that is, 2.9×10^{18} ^{6}He and 1.1×10^{18} ^{18}Ne decays per year [8]. This seems reasonable, as one does not expect loses with a refurbished SPS (to extrapolate, for instance, setup-I to setup-II at CERN). For the LHC one could compensate for injection loses due to the different optics with a different acceleration scheme with more or longer bunches (thus more ions) [24].

2.1. Neutrino fluxes

Neglecting small Coulomb corrections, the electron energy spectrum produced by an "allowed" nuclear $\beta-$decay at rest is described by:

$$\frac{dN^{\rm rest}}{dp_e} \sim p_e^2 (E_e - E_0)^2, \tag{2.1}$$

[8] Although the originally-projected intensity of ^{18}Ne was a factor three less, it was recently proposed [23] that three bunches could be accommodated.

where E_0 is the electron end-point energy and E_e and p_e are the electron energy and momentum. For ^{6}He, $E_0 = 3.5$ MeV $+ m_e$, while for ^{18}Ne, $E_0 = 3.4$ MeV $+ m_e$.

We are interested instead in the neutrino spectrum resulting from ion decays after they are boosted by some fixed γ. In the ion rest frame the spectrum of the neutrinos is

$$\frac{dN^{\rm rest}}{d\cos\theta dE_\nu} \sim E_\nu^2(E_0 - E_\nu)\sqrt{(E_\nu - E_0)^2 - m_e^2}. \tag{2.2}$$

After performing the boost and normalizing the total number of ion decays to be N_β per year, the neutrino flux per solid angle in a detector located at a distance L aligned with the straight sections of the storage ring is:

$$\left.\frac{d\Phi^{\rm lab}}{dSdy}\right|_{\theta\simeq 0} \simeq \frac{N_\beta}{\pi L^2}\frac{\gamma^2}{g(y_e)}y^2(1-y)\sqrt{(1-y)^2 - y_e^2}, \tag{2.3}$$

where $0 \le y = \frac{E_\nu}{2\gamma E_0} \le 1 - y_e$, $y_e = m_e/E_0$ and

$$g(y_e) \equiv \frac{1}{60}\left\{\sqrt{1-y_e^2}(2 - 9y_e^2 - 8y_e^4) + 15y_e^4 Log\left[\frac{y_e}{1-\sqrt{1-y_e^2}}\right]\right\} \tag{2.4}$$

Note the similarity of this expression and the electron neutrino fluxes at a neutrino factory [6]. Another similarity is that the fluxes are known very accurately and the $\nu_\mu(\bar\nu_\mu)$ appearance signal has no background from contamination of the beam. The latter is true for the neutrino factory only to the extent that the charge of final-state leptons can be determined, which requires, therefore, a magnetized device (thus, in particular it prevents the use of massive water detectors).

Figure 3 shows these fluxes at the three reference setups as a function of the neutrino energy. Although integrated fluxes for all the three setups are nearly identical, about $\mathcal{O}(10^{11})\bar\nu_e/\nu_e$ m^{-2} year^{-1}, setups II and III have the advantage that the appearance signal's energy dependence should be more significant, while at low energy the neutrino energy resolution is degraded by the Fermi motion.

It is instructive to compare with the neutrino factory flux of 10^{12} $\bar\nu_e/\nu_e$ m^{-2} year^{-1} at the optimum baseline of 3000 km. This is a factor 10 higher than setup II, but $\langle E_\nu\rangle/L$ for setups II and III is matched to the atmospheric splitting, while at the neutrino factory it is not. The oscillation probabilities are thus smaller in the latter.

2.2. Cross-sections

The (anti-)neutrino cross-sections relevant in the three setups are quite different. While in the low energy option quasi-elastic events are dominant and the cross-section grows rapidly with energy, in the highest-energy option samples are mostly deep-inelastic scattering and the growth is linear in the neutrino energy. For the medium-energy option, there is a sizable contribution from both types of events, as well as resonant channels. Figure 4 shows the cross-sections per nucleon and per neutrino energy used in this analysis.

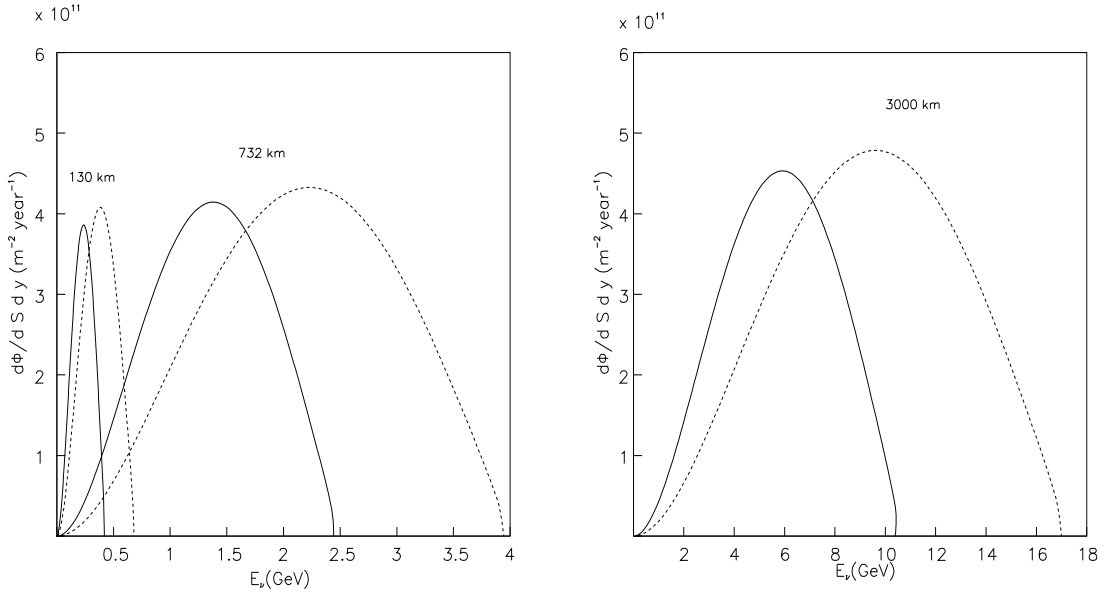

Figure 3: Fluxes for the three setups as function of the neutrino energy for $\bar{\nu}_e$ (solid) and ν_e (dashed).

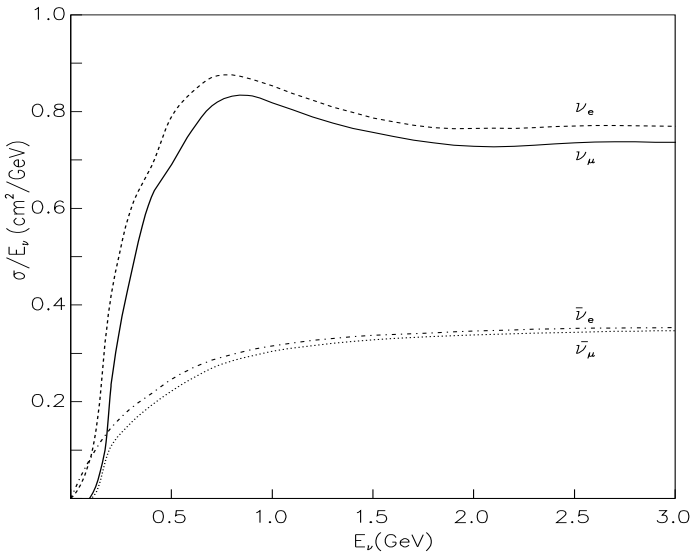

Figure 4: Cross section per nucleon for an isoscalar target, divided by neutrino energy in GeV.

γ	$L(km)$	$\bar{\nu}_e$ CC	ν_e CC	$\langle E_\nu \rangle (GeV)$
60/100	130	4.7	32.8	0.23/0.37
350/580	730	57.5	224.7	1.35/2.18
1500/2500	3000	282.7	993.1	5.80/9.39

Table 1: Number of charged-current events without oscillations per kton-year for the three reference setups. Also shown is the average neutrino energy.

Asymptotically the number of events grows linearly with γ. Table 1 shows the number of charged-current events expected in one year, per kiloton. The number of events is somewhat sensitive to the isotopic composition of the target, as free protons in water contribute significantly to the anti-neutrino event rates.

Interestingly, the detector mass can be reduced linearly with γ without changing the number of events. This offers the possibility of moving from the large water Cherenkov detector required in the lowest-energy option to a less massive but more granular detector in the higher-energy ones.

3. Detectors: efficiencies and backgrounds

The signature for the golden subleading transitions $\nu_e \to \nu_\mu$ and $\bar{\nu}_e \to \bar{\nu}_\mu$ in a β-beam is the appearance of prompt muons which must be separated from the main background of prompt electrons due to the bulk $\nu_e/\bar{\nu}_e$ charged interactions. Since there is only one neutrino species in the beam, no charge identification is required. Furthermore, to compensate the small cross sections, specially for setup-I, very massive detectors are needed. In addition, good energy resolution is required in order to resolve parameter degeneracies.

As demonstrated by Super-Kamiokande [1], massive water detectors are capable of offering simultaneoulsy excellent particle identification and good energy resolution, particularly in the range of few hundred MeV to about 1 GeV, where most of the interactions are quasi elastic, yielding simple event topologies (a typical QE interaccion is characterized by a single ring from the final muon, the scattered proton being below Cerenkov threshold thus invisible). As energy increases, deep inelastic processes start to dominate the cross section and the event topology becomes more complicated. The turn-over region is about 1.5 GeV. The neutrino spectra in Setup-II extend all the way up to 4 GeV. Nevertheless, as it will be shown below, water is still the best option in this range.

For neutrinos energies up to 10 GeV, as considered in setup-III, deep inelastic CC and NC events are dominant and water is no longer suitable. Massive tracking calorimeters are the best option in this range [25, 13].

3.1. Signal selection and background supression in water

We have considered a Megaton-class water detector, as proposed by the UNO collaboration [26] with a fiducial mass of 400 kiloton, for both setups I and II. The response of the detector was studied using the NUANCE [27] neutrino physics generator and detector simulation and realistic reconstruction algorithms as described in [9].

Particle identification in water exploits the difference in the Cerenkov patterns produced by showering ("e-like") and non-showering ("μ-like") particles. Besides, for the energies of interest the difference in Cerenkov opening angle between an electron and a muon can also be exploited. Furthermore, muons which stop and decay (100% of μ^+ and 78% of μ^-) produce a detectable delayed electron signature that can be used as an additional handle for background rejection.

For this study, we have used a particle identification criteria similar to the one used by the Super-Kamiokande collaboration, which is based on a maximum likelihood fit of both μ-like and e-like hypotheses. Figure 5 shows the particle identification estimator P_{id}, for electron-like events (solid line) and for muon-like events (dashed line). The normalization is arbitrary. A cut at $P_{id} > 0$ (PID cut) separates optimally the e-like and μ-like populations. Since most ν_μ events are followed by a muon-decay signature, the background is further reduced by accepting only events with a delayed coincidence.

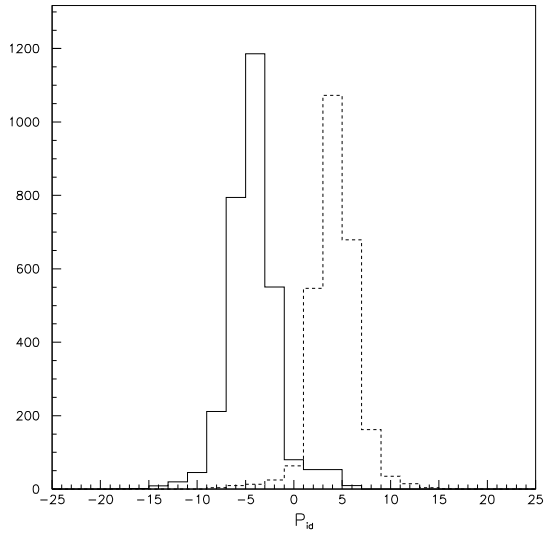

Figure 5: Rejection of ν_e^{CC} background in a water Cerenkov detector. The particle ID estimator $P_{\rm id}$ (in arbitrary units) is shown for the electron-like background (left, solid line) and muon-like signal (right, dashed).

To summarize, the event selection for both setup-I and setup-II requires:

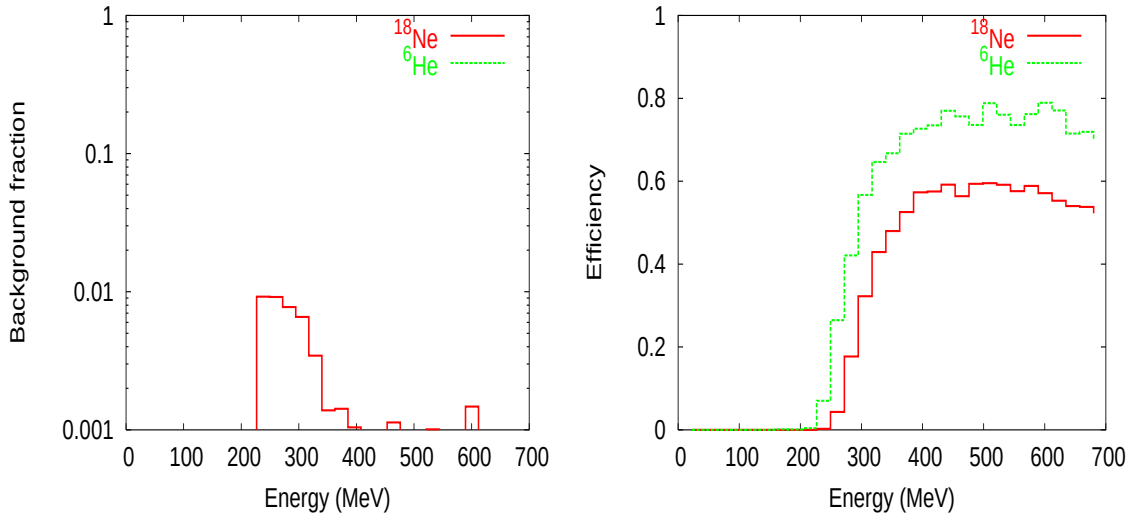

Figure 6: Background fraction (left) and efficiency (right) as a function of the true neutrino energies for ^{6}He and ^{18}Ne in water in Setup I.

- The event must be fully contained in the fiducial volume. This is necessary to guarantee a good measurement of the energy as well as to exploit the muon-decay signature.
- A single ring in the event.
- The PID estimator must be muon-like $P > 0$.
- Event must show a delayed coincidence (muon decay signature).

3.2. Signal and backgrounds in setup-I

The PID cut eliminates almost completely the electron background, leaving a residual background due to ν_e^{NC} and diffractive events in which a single pion is confused with a muon. The low energy of setup-I (particularly in the case of the antineutrinos) results in negligible backgrounds for ^{6}He. In the case of ^{18}Ne, diffractive events result in an integrated background fraction below 10^{-2}. The efficiency is rather large but drops dramatically below 300 MeV. Background ratio and efficiency as a function of the energy in setup-I are shown in Figure 6.

A major drawback of setup-I is that no energy binning is possible, since the neutrino energy is of the order of the Fermi motion. This is illustrated in Figure 7 where the reconstructed neutrino energy is plotted against the true energy. As it can be seen the events are almost uncorrelated. Therefore, spectral information cannot be used and one has to make do with the integrated signal, which, alas, cannot resolve the intrinsic degeneracies.

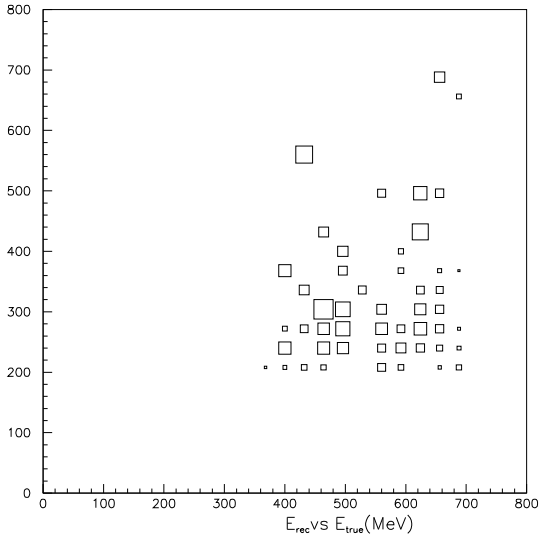

Figure 7: Reconstructed versus true neutrino energy for ^{18}Ne. The lack of correlation shows clearly that the event energy information is completely washed out by Fermi motion.

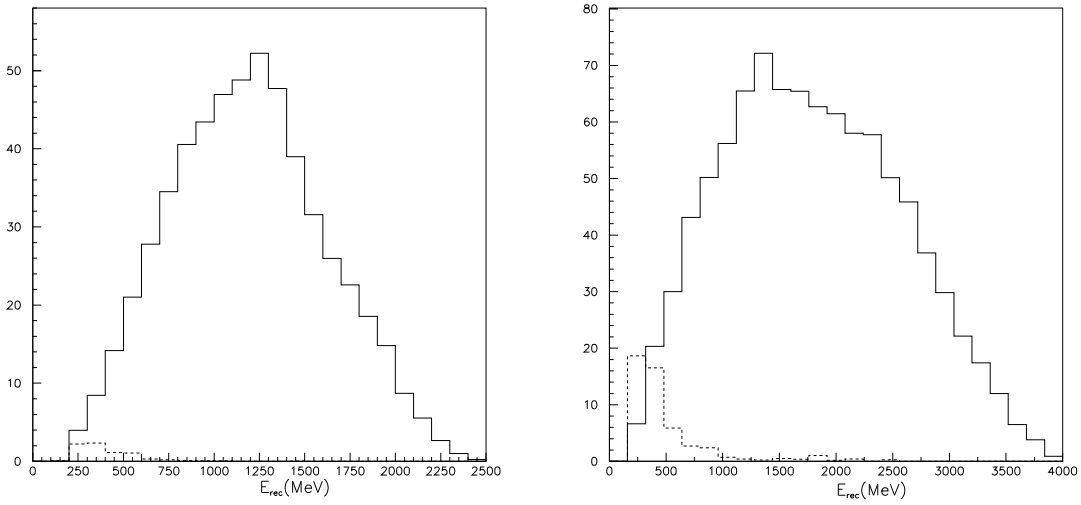

Figure 8: Reconstructed energy for signal and background in Setup-II (the absolute normalization is arbitrary) for ^{6}He (left) and ^{18}Ne (right).

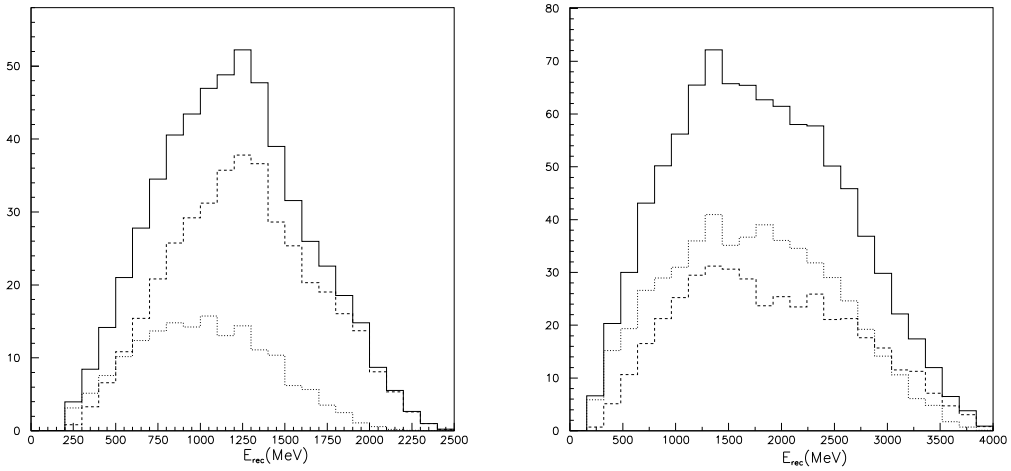

Figure 9: Reconstructed energy (solid line), the QE component (dotted line) and the non-QE component (dashed line) for signal-like events. (arbitrary normalization) for ^{6}He (left) and ^{18}Ne (right).

3.3. Signal and backgrounds in setup-II

Figure 8 shows the reconstructed energy spectrum for both signal and background in setup-II. Notice that, as for Setup-I, the backgrounds are smaller for ^{6}He than for ^{18}Ne, and that both neutrino and antineutrino backgrounds tend to cluster at low energies. A cut demanding that the reconstructed energy be larger than 500 MeV supresses most of the residual backgrounds at a modest cost for the efficiency.

Figure 9 shows the reconstructed energy (solid line), the QE component (dotted line) and the non-QE component (dashed line) for events passing the selection criteria. Notice that the non-QE contamination is high, specially for neutrino events. This spoils sizeably the resolution, since the neutrino energy is reconstructed under the hypothesis that the interaction was QE. The effect is ilustrated in Figure 10, which shows the reconstructed versus true energy for antineutrinos in Setup-II for QE events only (left) and all events (QE and non QE) that pass the selection criteria (right). Notice the excelent correlation between reconstructed and true energy in the case of QE events, which is, however, spoiled by the non-QE events. We take into account this effect by computing a matrix that describes the migrations between the true and the reconstructed neutrino energy. Migration matrices have also been computed for the backgrounds. Figures 11 and 12 show those matrices (in the form of lego-plots) for ^{6}He and ^{18}Ne respectively. The integrated efficiencies are quite high ($\sim 30 - 50\%$) for background fractions below 3×10^{-3}.

One possibility to control still better the backgrounds would be to have a tunable γ. In this way one could characterize the signal at a given energy reducing the background coming

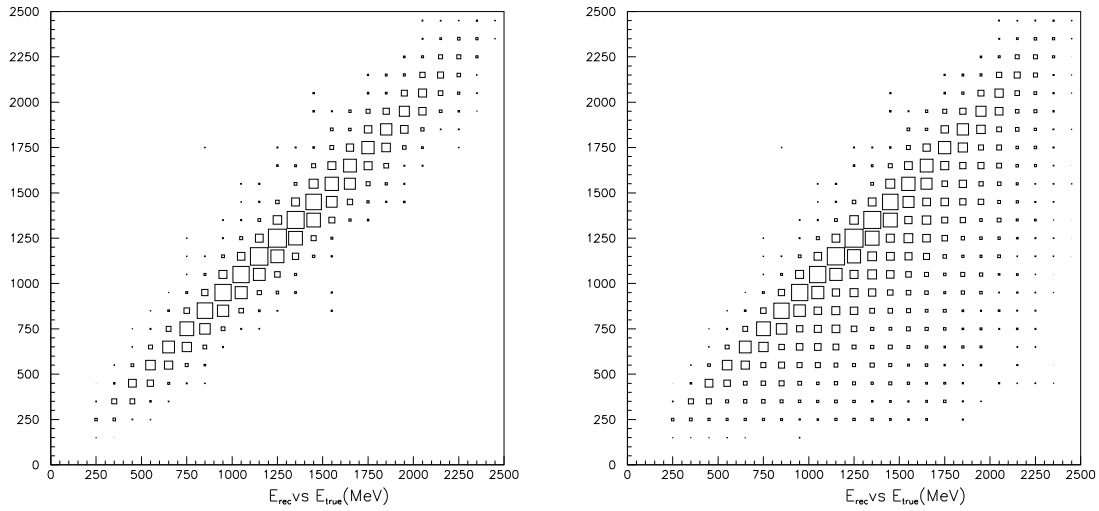

Figure 10: Reconstructed versus true energy for antineutrinos in Setup-II for QE events on the left and for signal-like events (QE and non-QE events) on the right.

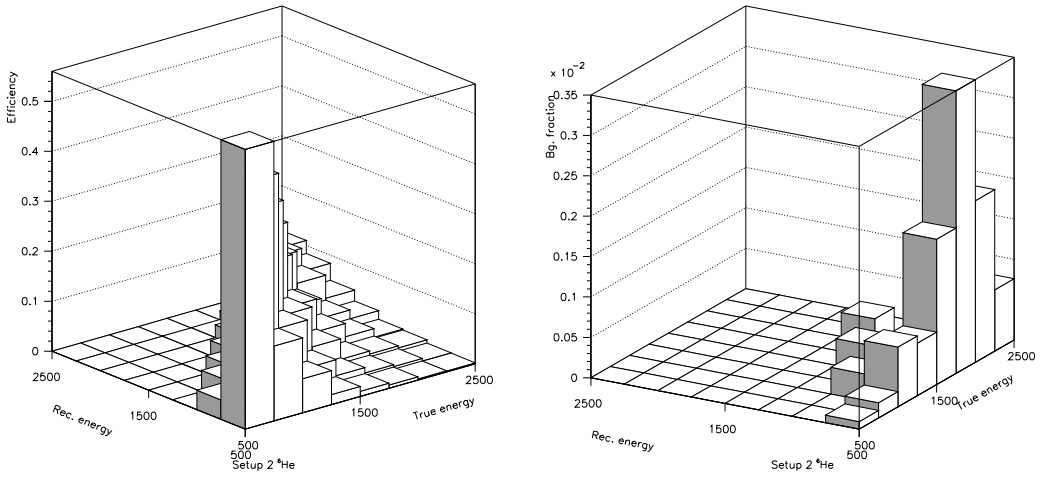

Figure 11: Efficiencies as a function of the true and reconstructed neutrino energies for ^{6}He in water in Setup II.

from higher energy events maximally. The optimization of such a design (how many years one should run at each γ) is an interesting one that will be considered elsewhere.

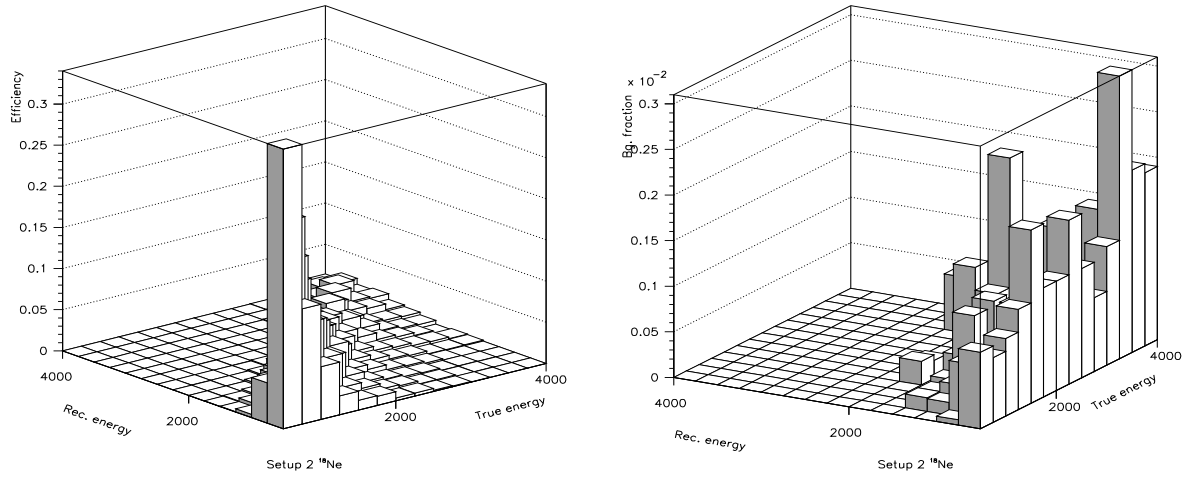

Figure 12: Efficiencies as a function of the true and reconstructed neutrino energies for ^{18}Ne in water for the case of Setup-II.

3.4. Setup-III

The neutrino spectra for setup-III extends up to a few GeV, well in the CC regime, where a tracking calorimeter (possibly a massive version of Minos [28]) could offer better performance than water. The performance of such a device (a 40 kiloton magnetized calorimeter) for the case of the neutrino factory has been extensively studied [25, 13]. However, the neutrino energy for that setup was higher (mean energy of about 25 GeV to compare with mean energy of about 5 GeV here) and the charge of the muon had to be measured, which is not the case here. We have not yet optimized the detector characteristics for the high energy option of the β-beam, but we expect a similar performance, with efficiencies better than 30 % and background fractions better than 10^{-4}. This will be the subject of a forthcoming study. In this paper, we will assume these numbers. We also assume that, as it was the case in [13], the neutrino energy can be reconstructed also for CC events. Energy bins of 1 GeV will be considered and we discard events with neutrino energies below 1GeV.

4. Determination of θ_{13} and δ

The simultaneous measurement of θ_{13} and δ is affected by correlations [13] and the so called *intrinsic* degeneracy [14], which results in either a proliferation of disconnected regions of parameter space, where the oscillation probabilities are very similar to be distinguished, or artificially large uncertainties in both parameters when these regions overlap.

As has been discussed before, these degeneracies can be resolved either combining different

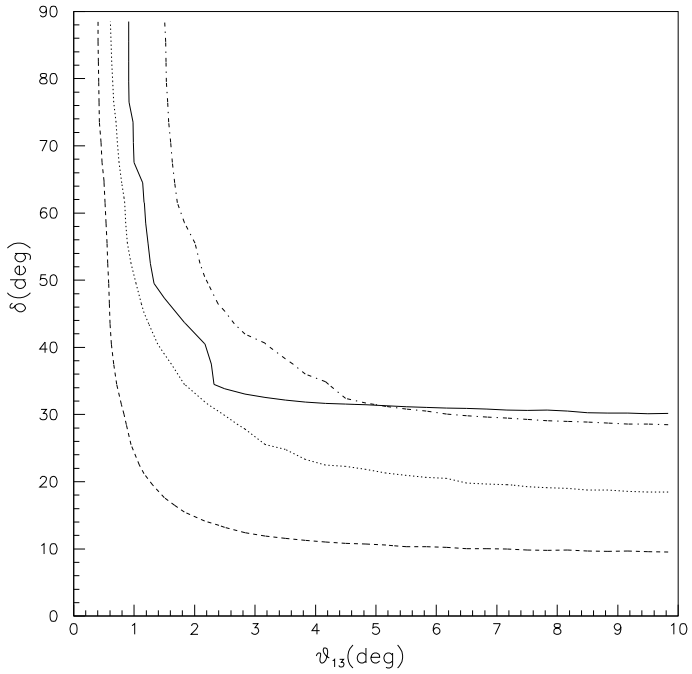

Figure 13: Region where δ can be distinguished from $\delta = 0$ or $\delta = 180^\circ$ with a 99% CL for setup I (solid), setup II with the UNO-type detector of 400 kton described in section 3.1 (dashed) and with the same detector with a factor 10 smaller mass (dashed-dotted) and setup III (dotted) with a 40 kton tracking calorimeter described in section 3.4. In all cases we consider 10 years of running time for both polarities (since they are accelerated simultaneously).

experiments with different E_ν/L or matter effects, or exploiting, whenever this is possible, the energy dependence of the signal within one experiment.

One of the main advantages of going to higher energies and longer baselines in the β-beam is precisely to have some significant energy resolution which allows to resolve these degeneracies.

In Figure 13 we compare the reach concerning CP-violation on the plane (θ_{13}, δ), i.e. the range of parameters where it is possible to distinguish with a 99%CL, δ from 0 or 180° for the different setups and 10 years of running in each case. We assume that both ions are bunched and accelerated simultaneously. We thus include the results from the measurement of both polarities. The remaining oscillation parameters are fixed close to their best fit values: $\Delta m^2_{23} = 2.5 \times 10^{-3}\text{eV}^2$, $\theta_{23} = 45^\circ$, $\Delta m^2_{12} = 7 \times 10^{-4}\text{eV}^2$, $\theta_{12} = 35^\circ$.

The solid line corresponds to the setup I, which has been studied before [12, 22]. The dashed lines correspond to setup II for the UNO detector described in the previous section

and for a detector scaled down by a factor of 10. Surprisingly the small water Cerenkov in setup II performs similarly to the UNO detector in setup I, while the performance of the latter in setup II is spectacular and clearly comparable with the neutrino factory. One of the reasons for this improvement is precisely the resolution of correlations. This can be seen in Fig. 14, where we compare the result of the fits for setups I, II and III. While the intrinsic degeneracies are present for the low-energy option, they tend to get resolved in the higher one, even with the smaller detector.

Notice that the necesity to supress backgrounds due to charge missidentification forces a very stringent cut in the momentum of the muon when searching for "wrong sign" muons at the neutrino factory [13]. This cut translates in practice in throwing away neutrino energies below 5 GeV, thus loosing precious spectral information. In that respect, the presence of two neutrino species in the neutrino factory is a disadvantage, compared with the $\beta-$beam, where one has only one neutrino species *and* the ability to identify low energy muons in water, separating them clearly from backgrounds (as opposed to a tracking calorimeter, where a muon of momentum less than about 1 GeV cannot be easily separated from the pion background).

Comparing setups II and III we realize that no improvement is gained at the highest γ as regards CP violation. The reason for this is probably the fact that matter effects become dominant at this longer baselines (see Fig. 1) and hide the genuine CP violation. Although an optimization of the detector design has not been performed in this case, it is clear that no gain will result with respect to setup II.

Although other systematic errors, such as the knowledge of the flux or the error on the backgrounds and efficiencies have not been included in this study, they are very unlikely to change the conclusion concerning the comparison of the three setups of the β-beam, since they would affect them in a similar manner. However *all* systematic errors should be included in a fair comparison of the β-beam and the neutrino factory, since they might be quite different in both machines.

5. Determination of the sign(Δm^2_{23})

The sign(Δm^2_{23}) is an essential missing piece of information to determine the structure of the neutrino mass matrix. The measurement of this quantity cannot be done from the measurement of neutrino oscillations in vacuum, so matter effects need to be sizable. In setup I, matter effects are too small to allow the determination of this unknown, however this is no longer the case for the intermediate baseline setup.

In Figure 15 we show the exclusion plot for the sign of Δm^2_{23} on the plane (θ_{13}, δ) at 99%CL. The measurement of the sign is possible in a very significant region of parameter space. In particular for the largest detector, it can be measured for $\theta_{13} \geq 4^\circ$, simultaneously with θ_{13} and δ ! On the other hand, in setup III the sign can be measured in a larger region

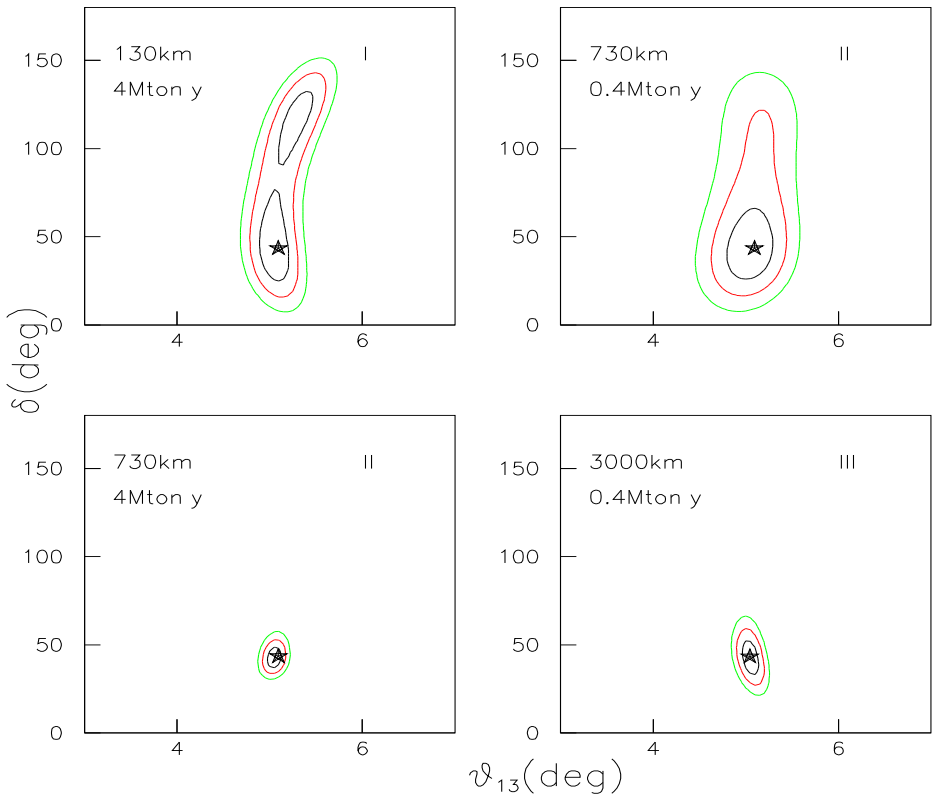

Figure 14: 1,2,3σ contours on the plane (θ_{13}, δ) in the setups I, II for the 40kton and 400 kton detectors and for setup III in 10 years of running time. The input values of the parameters are indicated by a star.

of parameter space. As discussed in the previous section this comes with the price that the sensitivity to CP violation gets spoiled.

6. Conclusions and Outlook

In this paper we have studied the physics potential of a higher γ β-beam and compared it with that of the present design ($\gamma \sim 100$, $L = 130$km). From a tecnical point of view, there does not seem to be any major difficulty in increasing the γ of the β-beam.

From the physics point of view the increase in γ is advantageous for three reasons: at the first atmospheric peak (which fixes γ/L) the rates increase linearly with γ, the increase in the baseline gives sizable matter effect, which allows to distinguish the sign of Δm^2_{23}, and

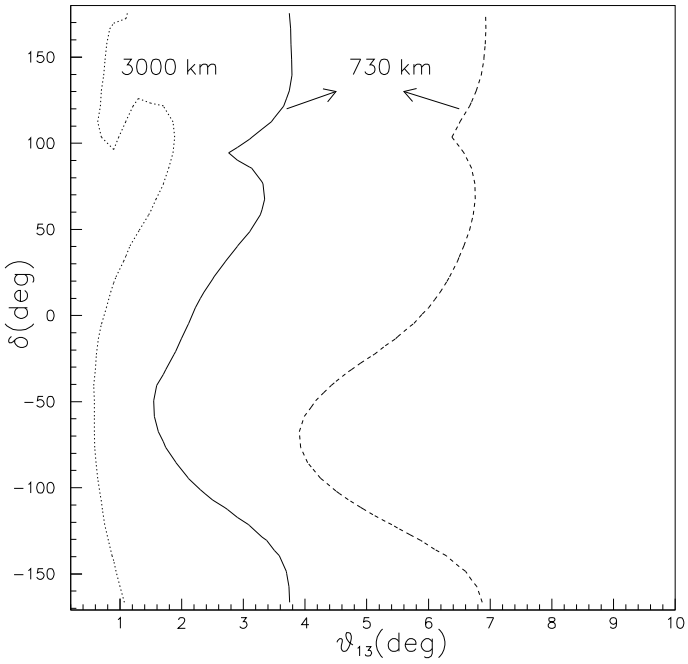

Figure 15: Regions where the true sign$(\Delta m^2_{23}) = +1$ can be measured at 99% CL (ie. no solution at this level of confidence exists for the opposite sign). The lines correspond to setup II with the 400kton water Cerenkov (solid), the 40kton one (dashed) and to setup III (dotted) in 10 years of running time.

finally the energy dependence of the oscillation signal is easier to measure and gives precious information to resolve correlations and degeneracies between oscillation parameters.

From the experimental point of view, a very important advantage of the low-energy option was the possibility to use a very massive water Cerenkov a la UNO, remains true if the γ is increased to $\gamma \sim 500$: the result of our realistic simulation shows that backgrounds can be reduced to a very small level with rather high efficiencies. At even higher energies water Cerenkov's are no longer optimal, but one could give up the increase in statistics by decreasing the detector mass, in such a way that a different technology, such as a calorimeter, can be used.

We have thus considered two reference higher γ options: $\gamma \sim 500$ and a water Cerenkov a la UNO at 730km and $\gamma \sim 2000$ with a 10 times smaller calorimeter (which is still to be optimized) at 3000km. Our results show that the intermediate γ option is spectacularly better than the low γ option previously considered, both in terms of the reach in CP violation as in the possibility to measure the neutrino mass hierarchy. The highest γ option instead

has an intermediate performance as regards the reach in CP violation. This is due to the fact that the baseline is so large that matter effects become dominant and hide to a large extent the genuine CP violation. On the other hand, the determination of the neutrino mass hierarchy is possible in a much enlarged region of parameter space.

In this study we have compared the different γ options alone. No combinations with possible super-beams or among themselves have been considered. Neither the interesting possibility to get the silver transition $\nu_e \to \nu_\tau$ in the highest energy options has been studied. The combination of golden and silver transitions has been shown to be extremely powerfull [19] in resolving degeneracies so this is an interesting question that will be addressed elsewhere.

In summary, we have shown that the perspectives as regards the physics reach of the β-beam are much more promising than previously thought, to the extent that it can become competitive with the neutrino factory [9]. In the light of these results, we believe that the high-γ option of a β-beam design deserves careful consideration. Note in particular that a β-beam, irrespective of the γ, does not require a proton driver with so much power as that required by the SPL super-beam or the neutrino factory.

Clearly a finer optimization of the γ(s) and baseline(s) to define an optimal roadmap for the β-beam complex requires a more detailed study (and also the better knowledge of the atmospheric and solar parameters that will be achieved in the next generation of neutrino experiments), but our results show that a γ in the range of $\mathcal{O}(500)$ with a megaton water Cerenkov at a distance $\mathcal{O}(1000\text{km})$ will be hard to beat.

Acknowledgement

We warmly thank A. Donini and S. Rigolin for usefull discussions and also M. Lindroos for his ideas on the feasibility of a higher energy β-beam and his encouragement. This work has been partially supported by FPA2002-00612 and FPA2001-1910/C03-02 of the CICYT and GV00-054-1.

[9] A fair comparision between the β-beam and the neutrino factory should however include a proper treatment of *all* systematic errors.

References

[1] Y. Fukuda *et al*, Phys. Rev. Lett **81** (1998) 1562.

[2] S. Fukuda *et al*, Phys. Rev. Lett.**86** (2001) 5651. Q.R. Ahmad *et al*, Phys. Rev. Lett **89** (2002) 011301 and 011302.

[3] M. Apollonio, *et al*, Eur. Phys. J. **C27** (2003) 331. K. Eguchi *et al*, Phys. Rev. Lett **90** (2003) 021802.

[4] M.H. Ahn, Phys. Rev. Lett **90** (2003) 041801.

[5] Z. Maki, M. Nakagawa and S. Sakata, Prog. Theor. Phys. **28** (1962) 970.

[6] S. Geer, Phys. Rev. **D57** (1998) 6989. A. De Rújula, M.B. Gavela and P. Hernández, Nucl. Phys. **B547** (1999) 21. For recent reviews see M. Apollonio, *et al*, arXiv:hep-ex/0210192; J. J. Gómez-Cadenas and D. A. Harris, Ann. Rev. Nucl. Part. Sci. **52** (2002) 253 the annual proceedings of the International Nufact Workshop.

[7] Y. Itow *et al*, Nucl. Phys. Proc. Suppl. **111** (2002) 146. [arXiv:hep-ex/0106019]

[8] A. Para and M. Szleper, arXiv:hep-ex/0110032; D. Ayres *et al*, arXiv:hep-ex/0210005.

[9] J. J. Gómez-Cadenas *et al.* [CERN working group on Super Beams Collaboration], arXiv:hep-ph/0105297.

[10] V. Martemyanov *et al*, arXiv:hep-ex/0211070; H. Minakata *et al*, arXiv:hep-ph/0211111; P. Huber *et al*, arXiv:hep-ph/0303232; O. Yasuda, arXiv:hep-ph/0309333.

[11] P. Zucchelli, Phys. Lett. **B532** (2002) 166.

[12] M. Mezzetto, J. Phys. **G.29** (2003) 1771 and 1781.

[13] A. Cervera *et al*, Nucl Phys. **B579** (2000) 17 [arXiv:hep-ph/0002108].

[14] J. Burguet-Castell *et al*, Nucl Phys. **B608** (2001) 301 [arXiv:hep-ph/0103258].

[15] H. Minakata and H. Nunokawa, JHEP **0110** (2001) 1, [arXiv:hep-ph/0108085].

[16] V. Barger, D. Marfatia and K. Whisnant, Phys. Rev. **D65** (2002) 073023, [arXiv:hep-ph/0112119].

[17] P. Huber, M. Lindner and W. Winter, Nucl. Phys.**B645** (2002) 3, [arXiv:hep-ph/0204352].

[18] J. Burguet-Castell *et al*, Nucl. Phys. **B646** (2002) 301, [arXiv:hep-ph/0207080].

[19] A. Donini, D. Meloni, P. Migliozzi, Nucl. Phys. **B646** (2002) 321, [arXiv:hep-ph/0206034]. D. Autiero *et al.*, arXiv:hep-ph/0305185.

[20] B. Autin *et al*, CERN/PS 2002-078 (OP), to be published in the proceedings of Nufact02 (London 2002) in J. Phys. G. For more references see also http://beta-beam.web.cern.ch/beta-beam/.

[21] B. Autin *et al*, CERN/PS 2002-012.

[22] J. Bouchez, M. Lindroos and M. Mezzetto, arXiv:hep-ex/0310059.

[23] M. Lindroos, talk at the Moriond Workshop on "Radioactive beams for nuclear physics and neutrino physics", http://moriond.in2p3.fr/radio/.

[24] M. Lindroos, private communication.

[25] A. Cervera, F. Dydak and J.J. Gómez-Cadenas, Nucl. Instrum. Methods **A 451** (2000) 123.

[26] M. Goodman, *et al*, "Physics Potential and feasability of UNO", ed. D. Casper, C.K. Jung, C. McGrew and C. Yanagisawa, SBHEP01-3 (July 2001).

[27] D. Casper, Nucl. Phys. Proc. Suppl. **112**(2002) 161 [arXiv:hep-ph/0208030].

[28] See http://www-numi.fnal.gov/.